Monthly Notices
of the
ROYAL ASTRONOMICAL SOCIETY

Mon. Not. R. Astron. Soc. **414,** 3281–3287 (2011) doi:10.1111/j.1365-2966.2011.18626.x

The *XMM–Newton* survey of the Small Magellanic Cloud: XMMU J005011.2−730026 = SXP 214, a Be/X-ray binary pulsar⋆

M. J. Coe,[1]† F. Haberl,[2] R. Sturm,[2] W. Pietsch,[2] L. J. Townsend,[1] E. S. Bartlett,[1] M. Filipovic,[3] A. Udalski,[4] R. H. D. Corbet,[5] A. Tiengo,[6] M. Ehle,[7] J. L. Payne[3] and D. Burton[8]

[1]*School of Physics and Astronomy, University of Southampton, Southampton SO17 1BJ*
[2]*Max-Planck-Institut für extraterrestrische Physik, Giessenbachstraße, 85748 Garching, Germany*
[3]*University of Western Sydney, Locked Bag 1797, Penrith South DC, NSW 1797, Australia*
[4]*Warsaw University Observatory, Aleje Ujazdowskie 4, 00-478 Warsaw, Poland*
[5]*University of Maryland, Baltimore County, Mail Code 662, NASA Goddard Space Flight Center, Greenbelt, MD 20771, USA*
[6]*INAF – Istituto di Astrofisica Spaziale e Fisica Cosmica – Milano, via E. Bassini 15, I-20133 Milano, Italy*
[7]*European Space Agency, XMM–Newton Science Operations Centre, PO Box 78, 28691 Villanueva de la Canada, Madrid, Spain*
[8]*University of Southern Queensland, Toowoomba, QLD 4350, Australia*

Accepted 2011 March 1. Received 2011 February 18; in original form 2011 January 13

ABSTRACT

In the course of the *XMM–Newton* survey of the Small Magellanic Cloud, a region to the east of the emission nebula N19 was observed in 2009 November. To search for new candidates for high-mass X-ray binaries, the EPIC-pn and EPIC-MOS data of the detected point sources were investigated and their spectral and temporal characteristics identified. A new transient (XMMU J005011.2−730026 = SXP 214) with a pulse period of 214.05 s was discovered; the source had a hard X-ray spectrum with a power-law index of ∼0.65. The accurate X-ray source location permits the identification of the X-ray source with an ∼15th magnitude Be star, thereby confirming this system as a new Be/X-ray binary.

Key words: stars: neutron – X-rays: binaries.

1 INTRODUCTION AND BACKGROUND

The Be/X-ray systems represent the largest sub-class of all high-mass X-ray binaries (HMXBs). A survey of the literature reveals that of the ∼240 HMXBs known in our Galaxy and the Magellanic Clouds (Liu, van Paradijs & van den Heuvel 2005, 2006), ≥50 per cent fall within this class of binary. In fact, in recent years it has emerged that there is a substantial population of HMXBs in the SMC comparable in number to the Galactic population. Though unlike the Galactic population, all except one of the Small Magellanic Cloud (SMC) HMXBs are Be star systems. In these systems the orbit of the Be star and the compact object, presumably a neutron star, is generally wide and eccentric. X-ray outbursts are normally associated with the passage of the neutron star close to the circumstellar disc (Okazaki & Negueruela 2001) and are generally classified as Type I or II (Stella, White & Rosner 1986). The Type I outbursts occur periodically at the time of the periastron passage of the neutron star, whereas Type II outbursts are much more extensive and occur when the circumstellar material expands to fill most or all of the orbit. This paper concerns itself with Type I outbursts. General reviews of such HMXB systems may be found in Negueruela (1998), Corbet et al. (2009), Coe (2000) and Coe et al. (2009).

One of the aims of the *XMM–Newton* large programme SMC survey (Haberl & Pietsch 2008a) is the ongoing study of the Be/X-ray binary population of the SMC, which can be used as a star formation tracer for ∼50 Myr old populations (Antoniou et al. 2010). In this paper, we present the analysis of X-ray and optical data from the newly discovered X-ray pulsar XMMU J005011.2−730026, hereafter referred to more simply as SXP 214 following the naming convention of Coe et al. (2005) for X-ray binary pulsars in the SMC.

2 X-RAY OBSERVATIONS

The Local Group galaxies are best suited to study their X-ray source populations using present-day observatories. Extending the existing archival observations, we have carried out a large programme in 2009 with *XMM–Newton* to obtain a complete X-ray survey of the SMC in the 0.1–10 keV band. The hard X-ray source SXP 214 that is the subject of this work was discovered as transient in observation 14 (Obs ID 0601211401 of the survey), on 2009 November 4. The

⋆Based on observations with *XMM–Newton*, an ESA Science Mission with instruments and contributions directly funded by ESA Member states and the USA (NASA).

†E-mail: mjcoe@soton.ac.uk

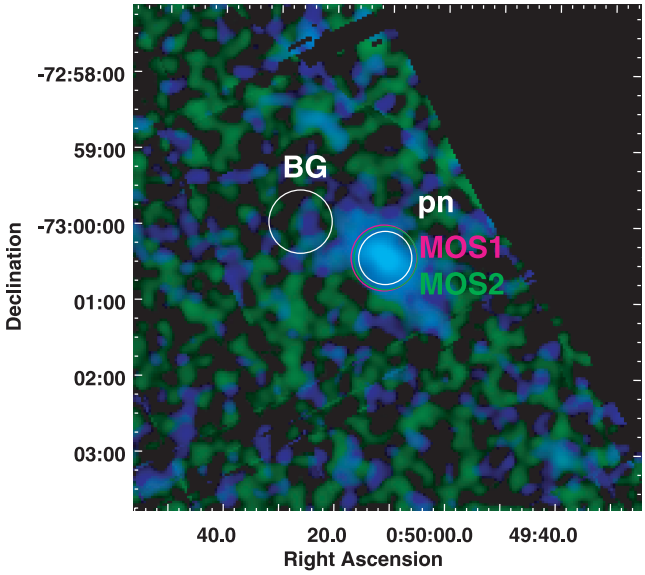

Figure 1. EPIC colour image of SXP 214 combining pn and MOS data. The red, green and blue colours represent the X-ray intensities in the 0.2–1.0, 1.0–2.0 and 2.0–4.5 keV energy bands, respectively. Circles indicate the extraction regions (with radii of 21, 26 and 25 arcsec for pn, MOS1 and MOS2 source regions and 25 arcsec for the background).

field is centred about 22 arcmin east of the emission nebula N19 in the south-western part of the SMC bar. It was observed by all three EPIC instruments (Strüder et al. 2001; Turner et al. 2001) at off-axis angles between 12.9 and 13.7 arcmin on CCDs 10, 3 and 4 for EPIC-pn, EPIC-MOS1 and EPIC-MOS2, respectively. All three cameras were operated in full-frame imaging mode with CCD readout frame times of 73 ms (pn) and 2.6 s (MOS). We used the *XMM–Newton* Science Analysis System (SAS) version 10.0.0[1] to reduce the data.

To correct the astrometric bore-sight, we identified eight sources (mainly known Be/X-ray binaries) in the field of view (FOV) with the Magellanic Clouds Photometric Survey of Zaritsky et al. (2002) and obtained a shift of ΔRA = 0.″10 and ΔDec. = 0.″70. The corrected X-ray position as found by emldetect is RA = $00^{h}50^{m}10\overset{s}{.}95$ and Dec. = –73°00′25.″0 (J2000.0), with a statistical error of 0.18 arcsec and a systematic uncertainty of ∼1 arcsec (1σ confidence for both cases). The relatively large systematic error is caused by the large off-axis angle of the source.

To remove times affected by background flares due to soft protons which occurred at the end of the observation (performed at the end of the satellite orbit), we defined good time intervals by applying thresholds to the background count rate in the 7.0–15.0 keV band of 8 and 2.5 counts ks^{-1} $arcmin^{-2}$ for EPIC-pn and EPIC-MOS, respectively. The soft proton background was at a very low level during the first part of the observation, thus resulting in net exposure times of 31.4 and 32.7 ks for EPIC-pn and EPIC-MOS, respectively.

To define extraction regions (see Fig. 1) for the source and background with an optimized signal-to-noise ratio, the SAS task eregion-analyse was used. We ensured that the source extraction region had a distance of >10 arcsec to other detected sources. For the background extraction, we defined a circular region covering the same point source free area on the sky for all three detectors. To avoid systematic detector background variations present close to CCD

[1] http://xmm.esac.esa.int/sas/

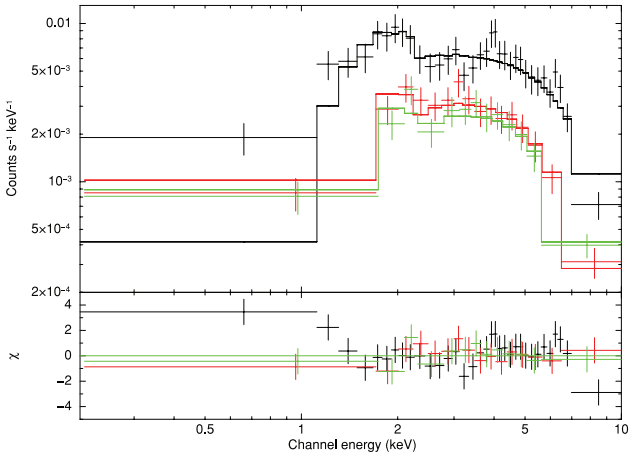

Figure 2. EPIC spectra of SXP 214. The top panel shows the EPIC-pn (black), EPIC-MOS1 (red) and EPIC-MOS2 (green) spectra together with the best-fitting model. The residuals are shown in the bottom panel.

borders where the source was located, we chose an area on the same CCDs as the source, and in the case of pn at a similar distance to the readout node. This restricted our selection to a radius of 25 arcsec. We extracted spectra, by selecting single- and double-pixel events from the EPIC-pn data and single-to-quadruple events from EPIC-MOS data, both with LAG = 0. The EPIC-pn/MOS1/MOS2 spectra contained 989/464/396 background-subtracted counts in the 0.2–10.0 keV band, respectively, and were binned to a minimum signal-to-noise ratio of 5 for each bin. To increase the statistics for the timing analysis, we also generated a merged event list from all three instruments, containing 2053 counts (source + background).

2.1 Spectral analysis

We used XSPEC (Arnaud 1996) version 12.6.0k for spectral fitting. The three EPIC spectra (see Fig. 2) were fitted simultaneously with a common set of spectral model parameters and a relative normalization factor for instrumental differences. The Galactic photoelectric foreground absorption was set to a column density of $N_{H,GAL} = 6 \times 10^{20}$ cm^{-2} with abundances according to Wilms, Allen & McCray (2000). The SMC column density was a free parameter with abundances for elements heavier than helium fixed at 0.2 (Russell & Dopita 1992). The emission was modelled with an absorbed power law where we obtained an SMC column density $N_{H,SMC} = (4.96 \pm 1.50) \times 10^{22}$ cm^{-2}, a photon index $\Gamma = 0.65 \pm 0.18$ and a flux in the 0.2–10.0 keV band of $(1.2 \pm 0.2) \times 10^{-12}$ erg cm^{-2} s^{-1}. Assuming a distance of 60 kpc, this corresponds to an unabsorbed luminosity of 7.1×10^{35} erg s^{-1}. The model resulted in an acceptable fit with χ^2/dof = 57/58, with relative normalization factors $c_{MOS1} = 1.18 \pm 0.13$ and $c_{MOS2} = 1.03 \pm 0.12$ (relative to $c_{pn} = 1$).

Since the EPIC-pn spectrum indicates a weak excess at ∼6.5 keV, we investigated a possible contribution of iron K emission lines at 6.4 keV (fluorescent emission) and 6.7 keV (Fe XXV) by assuming an unresolved linewidth. We obtained 90 per cent upper limits of 4.0×10^{-6} and 3.0×10^{-6} photons cm^{-2} s^{-1}, which correspond to equivalent width upper limits of 215 and 163 eV, respectively.

2.2 Timing analysis

The photon arrival times were randomized within the detector CCD frame time and recalculated for the Solar system barycentre using the SAS task barycen. We searched for pulsations in the X-ray light

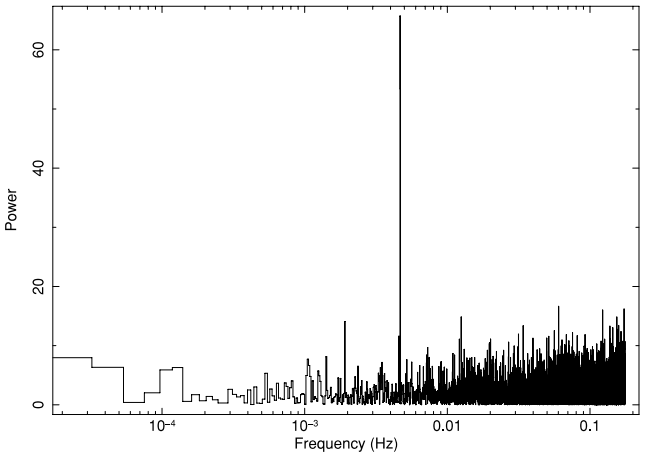

Figure 3. Power density spectrum created from the merged EPIC data in the 0.2–10.0 keV energy band. The time binning of the input light curve is 2.840 s.

curves in the EPIC standard energy bands (0.2–0.5, 0.5–1.0, 1.0–2.0, 2.0–4.5 and 4.5–10 keV) and combinations of them, using fast Fourier transform and light-curve folding techniques. The power density spectra derived from light curves in various energy bands from the different EPIC instruments showed a periodic signal at 0.004 67 Hz. To maximize the signal-to-noise ratio, we created light curves from the merged EPIC event list (filtered by the GTIs common to EPIC-pn and -MOS). Fig. 3 shows the inferred power density spectrum from the 0.2–10.0 keV energy band with the clear peak at a frequency of 0.004 67 Hz. Following Haberl, Eger & Pietsch (2008), we used a Bayesian periodic signal detection method (Gregory & Loredo 1996) to determine the pulse period with a 1σ error to (214.045 ± 0.052) s. In Fig. 4, pulse profiles folded with this period in different energy bands (based on the EPIC standard bands) are shown. Clear variations are seen above 1 keV, while due to the high absorption at lower energies the count rate is insufficient to detect a significant modulation. Hardness ratios were derived from the pulse profiles in two adjacent energy bands [$HR_i = (R_{i+1} - R_i)/(R_{i+1} + R_i)$ with R_i denoting the background-subtracted count rate in energy band i (with i from 1 to 4)]. Given the relatively low count rate, no significant hardness ratio variations are seen. We determined a pulsed fraction of (29 ± 9) per cent for the 0.2–10.0 keV band, assuming a sinusoidal pulse profile.

2.3 Long-term X-ray variability

The position of SXP 214 was observed with *XMM–Newton* three times before our large programme SMC survey, without any detection of the source. To derive upper limits, we used sensitivity maps of EPIC-pn and derived 3σ upper limits in the 0.2–10.0 keV band of 5.3×10^{-3} counts s^{-1} (Obs ID: 0110000101, 2000 October 15), 1.1×10^{-2} counts s^{-1} (Obs ID: 0404680101, 2006 October 5) and 4.1×10^{-3} counts s^{-1} (Obs ID: 0403970301, 2007 March 12). Assuming the best-fitting power-law spectrum from above, this corresponds to absorbed flux limits of 5.0×10^{-14}, 1.0×10^{-13} and 3.9×10^{-14} erg cm^{-2} s^{-1} or absorption-corrected luminosity limits of 2.5×10^{34}, 5.0×10^{34} and 1.9×10^{34} erg s^{-1}, respectively. The second limit is higher, due to a shorter background screened exposure of ∼7.7 ks, compared to ∼21 ks for the other two observations. The upper limits show that SXP 214 increased in brightness at least by a factor of 30 during its outburst.

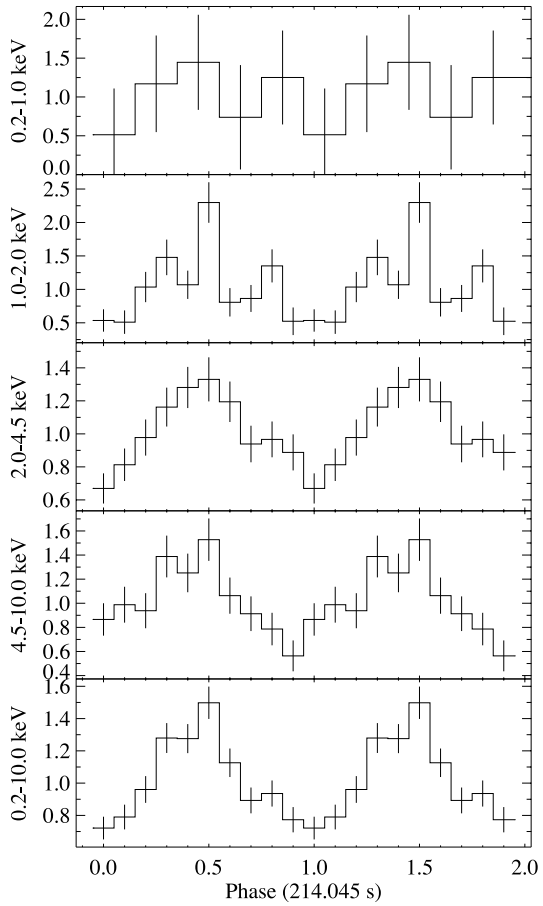

Figure 4. Pulse profiles obtained from the merged EPIC-pn/MOS1/MOS2 data in different energy bands (for better statistics, the first two standard energy bands were combined in the top panel; the bottom panel shows all five energy bands combined). The profiles are background-subtracted and normalized to the average count rate (0.0013, 0.0086, 0.027, 0.017 and 0.056 counts s^{-1}, from top to bottom).

SXP 214 has frequently fallen within the FOV of *RXTE* as part of the long-term monitoring of the SMC being carried out by some of the authors on this paper [see Galache et al. (2008) for a discussion of this campaign]. Though the collimator sensitivity to SXP 214 has been very high for periods of many months at a time, there are only eight possible detections with a confidence of ≥99 per cent at a high collimator response of ≥0.5 in over 10 yr. These detections are shown in Fig. 5. Unfortunately, the sparsity of these detections does not give us any significant insight into the binary period of this system neither do they reveal any obvious long-term spin period change.

The *RXTE* pulse amplitude may be converted to luminosity assuming a distance of 60 kpc to the SMC (though the depth of the sources within the SMC is unknown and *may* affect this distance by up to ±10 kpc). The X-ray spectrum was assumed to be a power law with a photon index = 1.5 and an $N_{\rm H} = 6 \times 10^{20}$ cm^{-2}. Furthermore, it was assumed that there was an average pulse fraction of 33 per cent for all the measurements and hence the correct total flux is three times the pulse component. Thus, the luminosity may be determined from the pulse amplitude values shown in Fig. 5 using the relationship

$$L_X = 0.4 \times 10^{37} \times 3R \,\mathrm{erg\,s^{-1}},$$

where R = pulsed amplitude counts in units of PCU^{-1} s^{-1}.

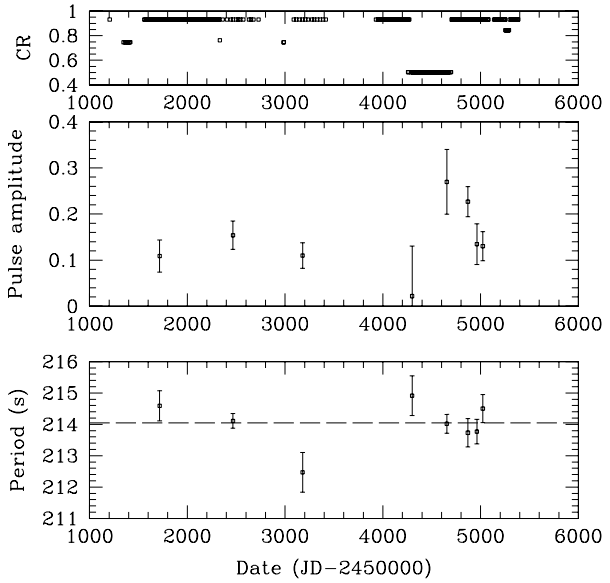

Figure 5. *RXTE* detections of SXP 214. The top panel shows the *RXTE* collimator response (CR) for the periods of time when this value exceeded 0.5. The middle panel shows the pulsed amplitude in counts $PCU^{-1}\ s^{-1}$ and the bottom panel shows the period detected. The dashed line in the bottom panel indicates the *XMM–Newton* period reported in this work.

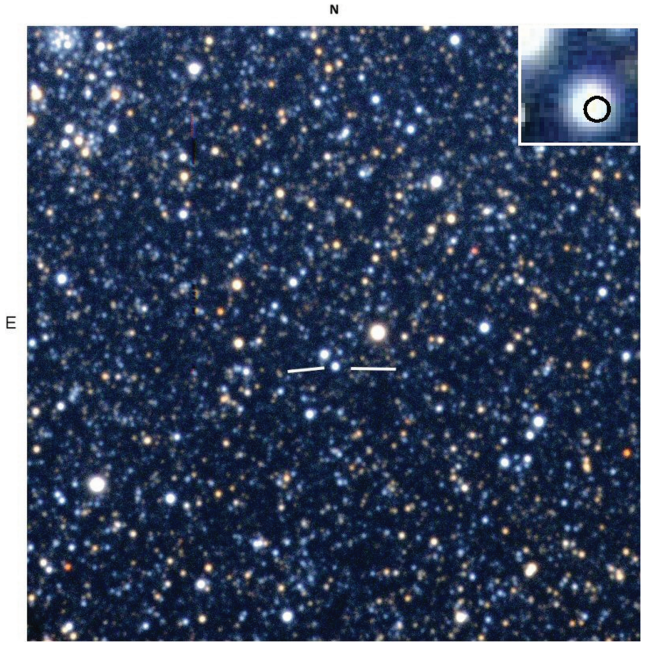

Figure 6. Finding chart for SXP 214 = XMMU J005011.2−730026. The colour image size is 5×5 arcmin^2 constructed from the *B*, *V* and *R* images taken with the Faulkes Telescope. The optical counterpart is indicated. An enlargement of the central 10×10 arcsec^2 is shown in the top-right corner, with the location and size of the X-ray error circle indicated.

The conclusion from the *RXTE* data is that there have been no major X-ray outbursts ($L_X \geq 10^{37}$ erg s^{-1}) over the last decade from SXP 214.

3 OPTICAL COUNTERPART

3.1 Optical and infrared photometry

From its precise X-ray position, the optical counterpart to SXP 214 is identified as SMC SC5 207965 in OGLE II and SMC 100.3 36998 in OGLE III (Udalski, Kubiak & Szymanski 1997) (see Fig. 6). It is also present in the massive compact halo object (MACHO) data as object 212.15966.18, but since these data significantly overlap in time with the OGLE II data, and are not taken through a standard *I*-band filter, they are not discussed any further. The long-term optical measurements of the counterpart to SXP 214 are presented in Fig. 7.

An extra *I*-band point was obtained as part of a set of *BVRI* observations made using the Faulkes Telescope on 25 November 2009 (MJD 55160), 21 d after the *XMM–Newton* detection reported here. The Faulkes Telescope is located at Siding Spring, Australia, and is a 2-m, fully autonomous, robotic Ritchey–Chretien reflector on an alt-azimuth mount. The telescope employs a robotic control system. The telescope was used in real-time interface mode for the observation of SXP 214. All the observations were pipeline-processed (flat-fielding and debiasing of the images). The magnitudes of the optical counterpart in all the observed bands were determined by comparison with several other nearby stars on the same image frame. In the case of the *I*-band stars from the OGLE data base, these comparison stars have not exhibited any significant variability in the last 8 yr of OGLE monitoring. In all other wavebands, reference stars from the catalogue of Massey (2002) were used.

The infrared (IR) counterpart is identified as Sirius 00501126−7300260 (Kato et al. 2007) and 2MASS 00501125−7300260. The

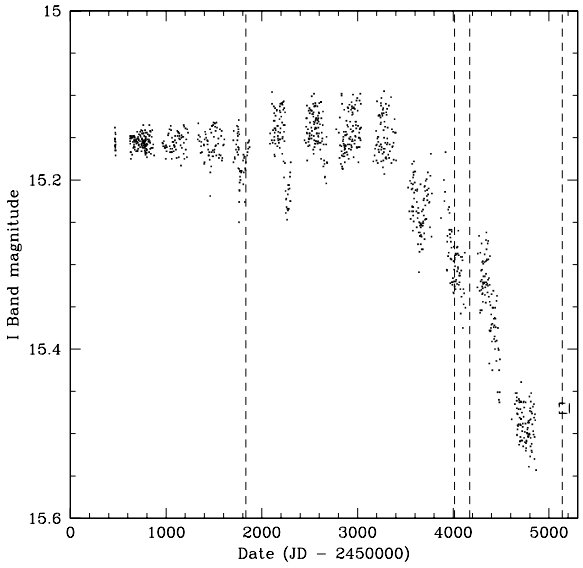

Figure 7. Optical *I*-band measurements of the counterpart to SXP 214 from OGLE II and III. The last point (open box) comes from the Faulkes Telescope taken on MJD 55160. The dates of the *XMM–Newton* observations are indicated by the vertical dashed lines – the source was not detected in the first three but just in the fourth observation (MJD 55139).

Sirius observations took place on 31 August 2002 and obtained the following results: $J = 15.32 \pm 0.02, K = 15.37 \pm 0.02$. New measurements in the *J*, *H* and *K* photometric bands were obtained on 2009 December 11 (MJD 55176) with the same Sirius camera on the 1.4-m IRSF telescope in South Africa (Kato et al. 2007). The full set of photometric measurements is shown in Table 1 and reveal that the IR magnitudes are fainter by ∼0.3 at the time of the *XMM–Newton* detection compared with the catalogue numbers.

Table 1. Optical and IR photometric measurements of SXP 214 taken in 2009 November and December (see the text for details).

Waveband	Magnitude	Error on magnitude
B	15.22	0.02
V	15.33	0.02
R	15.47	0.01
I	15.47	0.03
J	15.67	0.02
H	15.55	0.03
K	15.61	0.09

The $(B - V)$ colour index obtained from our data is $(B - V) = -0.11 \pm 0.03$. Correcting for an extinction to the SMC of $E(B - V) = 0.09$ (Schwering & Israel 1991) gives an intrinsic colour of $(B - V) = -0.20 \pm 0.03$. From Wegner (1994), this indicates a spectral type in the range B1V–B3V, typical of optical counterparts to Be/X-ray binaries in the SMC (McBride et al. 2008). However, care must always be taken when interpreting colour information as a spectral type in systems that clearly have circumstellar discs. Such discs can make significant contributions to the *B* and *V* bands.

The OGLE III data were detrended using a polynomial function and then subjected to a period search in the range of 2–200 d. Longer periods are harder to explore because they tend to approach the length of each data block (∼200 d) and the annual observing cycle. Two strong adjacent peaks emerged in the power spectrum (see Fig. 8). These peaks are at 4.520 and 4.576 d, respectively. According to the Corbet diagram for the SMC sources (Corbet et al. 2009), it is very unlikely that SXP 214 could have a binary period of this order. In fact, one of the two peaks (4.576 d) appears to be a beat period between the other period and the annual sampling of the OGLE III data. This is confirmed by examining just 1 yr of the data set which reveals just the one peak at 4.520 d. Furthermore, if this period does not represent a binary period, then the most likely explanation is that it is a non-radial pulsation (NRP) within the Be star (Diago et al. 2008) or, perhaps, the beat of the true NRP period with the daily sampling.

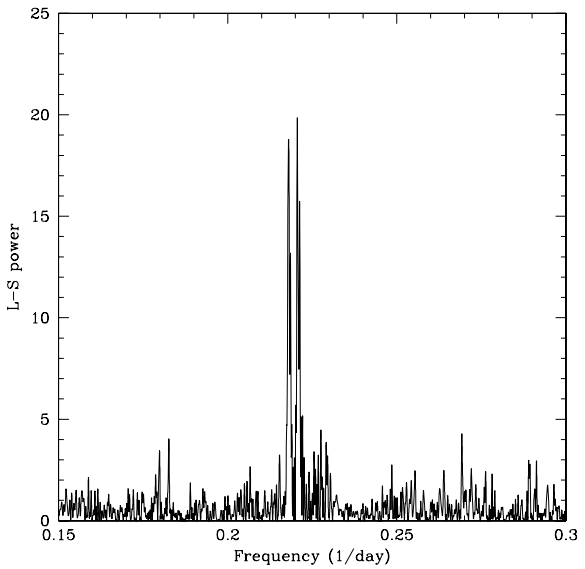

Figure 8. Lomb–Scargle power spectrum of the OGLE III data set.

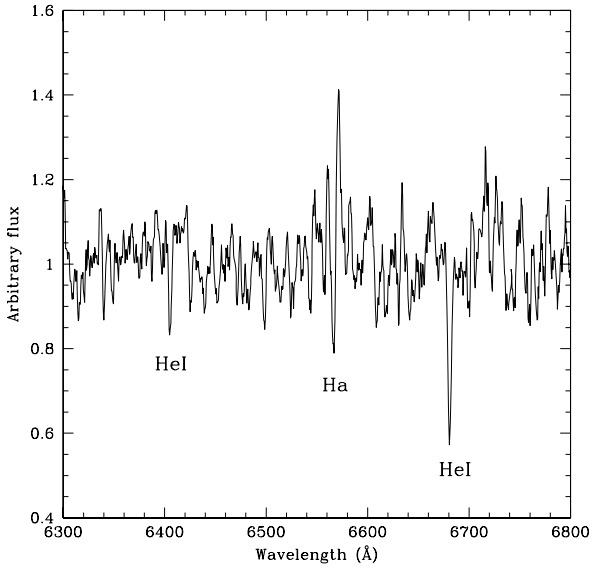

Figure 9. Optical spectrum of the region around Hα. The most obvious line features are indicated.

3.2 Optical spectroscopy

Spectroscopic observations of the Hα region were made on 11 December 2009 (MJD 55176) using the 1.9-m telescope of the South African Astronomical Observatory (SAAO). A 1200 lines per mm reflection grating blazed at 6800 Å was used with the SITe CCD which is effectively 266×1 798 pixels in size, creating a wavelength coverage from 6200 to 6900 Å. The intrinsic resolution in this mode was 0.42 Å pixel^{-1}. The spectrum resulting from a 2000-s integration is shown in Fig. 9.

The signal-to-noise ratio is poor in this spectrum, but there is definite evidence for a weak feature around Hα. An Hα line emission width of -1.5 ± 1.0 Å is estimated. Higher quality data are definitely required to establish if the line shows any structure. Absorption-line features associated with He I at rest wavelengths of 6406 and 6676 Å are also marked in the figure.

Additional observations were made using the integral field spectroscopy (IFS) instrument on 2010 December 28 at Siding Springs Observatory using the 2.3-m Advanced Technology Telescope and its Wide Field Spectrograph (WiFeS). The 1200-s single exposure was made in the central region of SXP 214 at a position angle (east of north) of 0° under clear skies with seeing estimated at 1 arcsec. The exposure was made in classical equal mode using the RT560 beam splitter and 3000 volume phased holographic gratings. For these gratings, the blue (708 lines mm^{-1}) range included 3200–5900 Å. The data were reduced using the WiFeS data reduction pipeline based on National Optical Astronomy Observatory IRAF software. This data reduction package was developed from the Gemini IRAF package (McGregor et al. 2003). Use of the pipeline consists of four primary tasks: wifes to set environment parameters; wftable to convert single extension FITS file formats to multi-extension FITS ones and create file lists used by subsequent steps; wfcal to process calibration frames including bias, flat-field, arc and wire; and wfreduce to apply calibration files and create data cubes for analysis. Using QFitsView3,[2] a spectrum of SXP 214 in the blue range was created and is shown in Fig. 10.

[2] Written by Thomas Ott and freely available at www.mpe.mpg.de/ott/dpuser/index.html

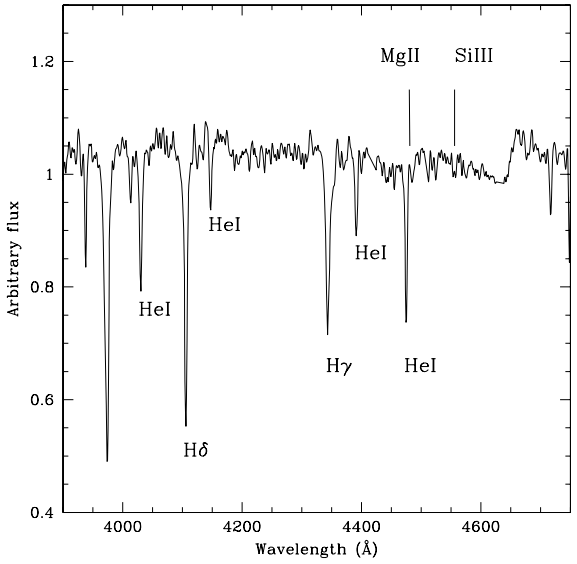

Figure 10. Optical spectrum of the spectral classification region.

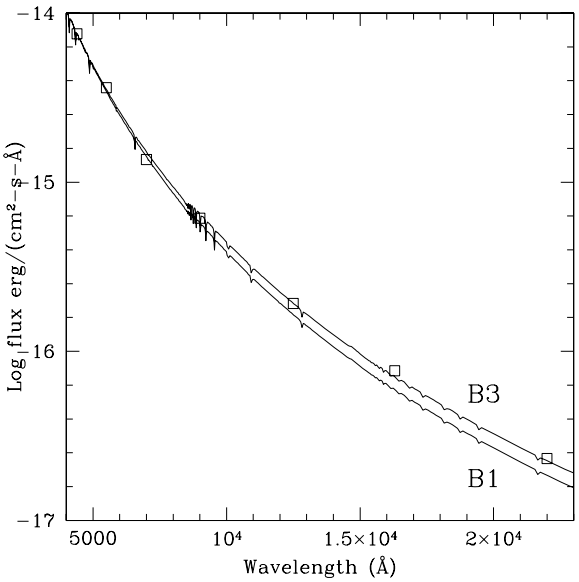

Figure 11. Optical and IR photometry (*BVRIJHK*) dereddened with $E(B-V) = 0.09$ and compared with the Kurucz model atmospheres for B1V and B3V stars. The model atmospheres have been normalized to the *B*-band point.

4 DISCUSSION AND CONCLUSIONS

During the *XMM–Newton* survey of the SMC, we discovered a new hard X-ray transient with a 0.2–10 keV luminosity of 7×10^{35} erg s^{-1}. The precise position derived from the EPIC data allowed us to identify a $V = 15.3$ mag early-type star as an optical counterpart. An optical spectrum taken at SAAO revealed a weak Hα line which clearly identifies the source as a Be/X-ray binary in the SMC. After SXP 11.87, this is the second discovery of such a system during the *XMM–Newton* SMC survey (Sturm et al. 2011).

SXP 214 shows X-ray pulsations with a period of 214.05 s and a hard (power-law) X-ray spectrum (photon index of ∼0.65). Conspicuous are the residuals in the EPIC-pn spectrum at low energies (≤1.5 keV; see Fig. 2). This might be caused by instrumental differences at high off-axis angles or by the contribution of a soft excess (Hickox, Narayan & Kallman 2004). In the latter case, the low count rate and the high absorption do not allow us to fit an additional component. We note that a soft excess originating near the neutron star (accretion column or disc) and absorbed by the same high column density as the power-law component would require an unrealistic high luminosity of $L \sim 10^{39}$ erg s^{-1} to cause this signal. Therefore, if a soft spectral component exists, it more likely originates in an optically thin gas cloud around the neutron star attenuated by much lower absorption. Given the relatively low outburst luminosity of SXP 214, this is consistent with the conclusions about the origin of soft excesses in the spectra of HMXBs drawn by Hickox et al. (2004).

At the time of this *XMM–Newton* detection and other related observations, the source seems to be in an optical low state compared with the past decade. In addition, the three previous *XMM–Newton* observations of SXP 214 have upper limits at least a factor of 10 below the flux level reported here (7×10^{35} erg s^{-1}). So at first glance it seems strange that it was finally detected by *XMM–Newton* when the optical flux was at such a low point. However, placing SXP 214 on the Corbet diagram would suggest a binary period of the order of 100–200 d. It is therefore very probable that the previous observations failed to catch the system with the neutron star at periastron and hence missed any Type I outbursts that may have occurred. The long-term *RXTE* monitoring (Fig. 5) at a good collimator sensitivity clearly shows the lack of any more prolonged (≥1 month) Type II outbursts from this system.

Not only is the *I*-band flux at a very low value for this system, but the Hα equivalent width also implies that a very minimal circumstellar disc was present in late 2009. If Kurucz model atmospheres (Kurucz 1979) representing the proposed spectral class range (B1V–B3V) are normalized to the dereddened *B*-band flux [using $E(B-V) = 0.09$ from Schwering & Israel (1991)], it again becomes clear that there is very little evidence for any substantial IR excess arising from a circumstellar disc (see Fig. 11). So anything from B1V with a small disc to B3V with essentially no disc at all offers a satisfactory fit to all the optical and IR data.

A more precise spectral classification may be determined from Fig. 10. Following the method given in Evans et al. (2004), an absence of He I λλ4200, 4541 lines defines the class to be later than B0. The weak but approximately equal strength of Mg II (λ4481) and Si III(λ4553) narrows it down to B2.5, though it could be up to half a class on either side. In the context of the luminosity class, if we take the *V*-band magnitude presented here and correct for the distance modulus (18.9) and the extinction to the SMC [$E(B-V) = 0.08$], an absolute magnitude of −3.83 results. Comparing this to the data in Wegner (1994) predicts a luminosity class III for a B2 star. So the best spectral identification from the data presented here gives B2–B3 III, which adds further support to a minimal circumstellar disc in this system.

In contrast, the column density derived from the X-ray spectrum of $\sim 5 \times 10^{22}$ cm^{-2} is relatively high for Be/X-ray binaries in the SMC (see fig. 12 in Haberl et al. 2008) and largely exceeds the total SMC H I column density of 1.1×10^{22} cm^{-2} (Stanimirovic et al. 1999). This suggests a large amount of source-intrinsic absorption close to the neutron star or that the line of sight to the X-ray source during the *XMM–Newton* observation passed close to the Be star, implying a large system inclination. An even more extreme case is the Be/X-ray binary pulsar SXP 1323 = RX J0103.6−7201 presented by Eger & Haberl (2008). During one of more than 20 *XMM–Newton* observations of RX J0103.6−7201 the absorption

exceeded 10^{23} cm^{-2}, completely suppressing the hard power-law component at energies below 2 keV and revealing a strong soft spectral component, likely caused by reprocessing in optically thin gas. In the case of SXP 214, this soft component is much weaker, consistent with the above conclusion hat only a minimal circumstellar disc was present during the *XMM–Newton* observation. It is worth noting that within our galaxy columns of up to 10^{24} cm^{-2} have been measured for some highly obscured HMXB systems.

ACKNOWLEDGMENTS

RS acknowledges support from the BMWI/DLR grant FKZ 50 OR 0907. LJT is supported by a University of Southampton Mayflower Scholarship. As always, we are grateful to the support staff in SAAO for help in using the 1.9-m and IRSF telescopes. The Faulkes Telescope Project is an educational and research arm of the Las Cumbres Observatory Global Telescope Network (LCOGTN). The OGLE project has received funding from the European Research Council under the European Community's Seventh Framework Programme (FP7/2007-2013)/ERC grant agreement no. 246678 to AU. MF thanks Australian Government AINSTO AMNRF for grant number 10/11-O-06.

REFERENCES

Antoniou V., Zezas A., Hatzidimitriou D., Kalogera V., 2010, ApJ, 716, L140
Arnaud K. A., 1996, in Jacoby G. H., Barnes J., eds, ASP Conf. Ser. Vol. 101, Astronomical Data Analysis Software and Systems V. Astron. Soc. Pac., San Francisco, p. 17
Coe M. J., 2000 in Smith M. A., Henrichs H. F., eds, ASP Conf. Ser. Vol. 214, The Be Phenomenon in Early-Type Stars. Astron. Soc. Pac., San Francisco, p. 656
Coe M. J., Edge W. R. T., Galache J. L., McBride V. A., 2005, MNRAS, 356, 502
Coe M. J. et al., 2009, in van Loon J., Oliveira J. M., eds, Proc. IAU Symp. 256, The Magellanic System: Stars, Gas, and Galaxies. Kluwer, Dordrecht, p. 367
Corbet R. H. D., Coe M. J., McGowan K. E., Schurch M. P. E., Townsend L. J., Galache J. L., Marshall F. E., 2009, in van Loon J., Oliveira J. M., eds, Proc. IAU Symp. 256, The Magellanic System: Stars, Gas, and Galaxies. Kluwer, Dordrecht, p. 361
Diago P. D., Gutiérrez-Soto J., Fabregat J., Martayan C., 2008, A&A, 480, 179
Eger P., Haberl F., 2008, A&A, 491, 841
Evans C. J., Howarth I. D., Irwin M. J., Burnley A. W., Harroes T. J., 2004, MNRAS, 353, 601
Galache J. L., Corbet R. H. D., Coe M. J., Laycock S., Schurch M. P. E., Markwardt C., Marshall F. E., Lochner J., 2008, ApJS, 177, 189
Gregory P. C., Loredo T. J., 1996, ApJ, 473, 1059
Haberl F., Pietsch W., 2008, in Carpano S., Ehle M., Pietsch W., eds, X-rays From Nearby Galaxies. MPE Report 295, Germany, p. 32
Haberl F., Eger P., Pietsch W., 2008, A&A, 489, 327
Hickox R. C., Narayan R., Kallman T. R., 2004, ApJ, 614, 881
Kato D. et al., 2007, PASJ, 59, 615
Kurucz R. L., 1979, ApJS, 40, 1
Liu Q. Z., van Paradijs J., van den Heuvel E. P. J., 2005, A&A, 442, 1135
Liu Q. Z., van Paradijs J., van den Heuvel E. P. J., 2006, A&A, 455, 1165
McBride V. A., Coe M. J., Negueruela I., Schurch M. P. E., McGowan K. E., 2008, MNRAS, 388, 1198
Massey P., 2002, ApJS, 141, 81
McGregor P. J. et al., 2003, in Masanori I., Moorwood A. F. M., eds, Proc. SPIE 4841, Instrument Design and Performance for Optical/Infrared Ground-based Telescopes. SPIE, Bellingham, p. 1581
Negueruela I., 1998, A&A, 338, 505
Okazaki A. T., Negueruela I., 2001, A&A, 377, 161
Russell S. C., Dopita M. A., 1992, ApJ, 384, 508
Schwering P. B. W., Israel F. P., 1991, A&A, 246, 231
Stanimirovic S., Stavely-Smith L., Dickey J. M., Sault R. J., Snowden S. L., 1999, MNRAS, 302, 417
Stella L., White N. E., Rosner R., 1986, ApJ, 308, 669
Strüder L. et al., 2001, A&A, 365, L18
Sturm R. et al., 2011, A&A, 527, 131
Turner M. J. L. et al., 2001, A&A, 365, L27
Udalski A., Kubiak M., Szymanski M., 1997, Acta Astron., 47, 319
Wegner W., 1994, MNRAS, 270, 229
Wilms J., Allen A., McCray R., 2000, ApJ, 542, 914
Zaritsky D., Harris J., Thompson I. B., Grebel E. K., Massey P., 2002, AJ, 123, 855

This paper has been typeset from a TEX/LATEX file prepared by the author.